ELSEVIER

S0032-3861(96)00444-2

Polymer Vol. 37 No. 26, pp. 5907–5916, 1996

0032-3861/96/$15.00+0.00

Emulsion polymerization: particle growth kinetics

Lourdes López de Arbina, María J. Barandiaran, Luis M. Gugliotta* and José M. Asua†

Grupo de Ingeniería Química, Departamento de Química Aplicada, Facultad de Ciencias Químicas, Universidad del País Vasco/Euskal Herriko Unibertsitatea, Apdo. 1072, 20080 San Sebastián, Spain

(Received 24 October 1995; revised 5 February 1996)

An attempt to develop a predictive and manageable mathematical model for particle growth in emulsion homopolymerization was carried out by fitting the time evolution of the conversion in the chemically initiated seeded emulsion polymerization of styrene carried out under a wide range of experimental conditions with models of different complexity. Model discrimination based on the best fitting of the experimental data was carried out. No advantage was gained by increasing the complexity of the mathematical model. The dependence of the radical entry and exit rate parameters on the particle size was used to elucidate between the different mechanisms proposed for these processes. Copyright © 1996 Elsevier Science Ltd.

(Keywords: emulsion polymerization; kinetics; entry)

INTRODUCTION

One important goal in the investigation of the emulsion polymerization processes is the development of predictive mathematical models. In order to be predictive, the mathematical model should be based on the fundamental mechanisms involved in the process. However, emulsion polymerization is a complex multiphase reaction system in which polymerization proceeds according to a rather complicated kinetic scheme. It is possible to develop a complete mathematical model including all the details that one can imagine, but this risks being a sterile exercise because it may be impossible to design experiments able to provide enough information to both discriminate the mechanisms that actually occur and estimate the corresponding parameters. In addition, complex models are difficult to use in some applications such as on-line control. On the other hand, the range of application of too-simple models is restricted to the range of experimental conditions in which the experiments used to estimate the parameters of these models were carried out, i.e. they have a very limited predictive capability. Therefore, the mathematical model has to be both predictive and manageable.

This paper is an attempt to develop such a model for particle growth in emulsion polymerization. To achieve this goal, mathematical models of different levels of complexity were used to fit the time evolution of the conversion during the approach to the steady state value of the average number of radicals per particle, $\bar{n}$, in the chemically initiated seeded emulsion polymerization of styrene carried out under a wide range of experimental conditions. Model discrimination based on the best fit of the experimental data was carried out. The mathematical models include rate coefficients for radical entry and exit for which different mechanisms have been proposed[1–12]. The dependence of the estimated values of these parameters on the particle size was used to elucidate between the different mechanisms.

MATHEMATICAL MODELS

The events involved in an emulsion polymerization initiated with a water-soluble thermal initiator are as follows[13]: (i) generation of free radicals by decomposition of the initiator in the aqueous phase and to some extent by the 'background' thermal process[12]; (ii) propagation of the free radicals in the aqueous phase; (iii) termination of free radicals in the aqueous phase; (iv) entry of free radicals into the latex particles; (v) desorption of the free radicals from the polymer particles; (vi) propagation within the polymer particles; (vii) termination within the polymer particles.

In these events, free radicals with different chain lengths and different chemical compositions, according to whether they arise from the initiator or from a desorbed radical, are involved. The complexity of the mathematical model depends on the level of description of these radicals. In this work, different mathematical models have been used.

Model 1

The simplest model (Model 1) makes no distinction between radicals in the aqueous phase, considering that all of them have the same probability for propagation, termination and entry. A detailed discussion about this

*On leave from INTEC (Consejo Nacional de Investigaciones Científicas y Técnicas and Universidad Nacional del Litoral, Santa Fe, República Argentina)

† To whom correspondence should be addressed

model is provided in ref. 13. The monomer material balance for an emulsion homopolymerization carried out in a batch reactor, under conditions such as the contribution of the aqueous phase polymerization to the overall conversion is negligible and the 'zero–one' assumption holds, is as follows:

$$\frac{dx}{dt} = \frac{k_p[M]_p N_1}{M_0 N_A} \quad (1)$$

where x is the fractional conversion of the monomer, k_p the propagation rate constant in the polymer particles, $[M]_p$ the concentration of the monomer in the polymer particles, N_1 the number of particles per cm^3 of water containing 1 radical, M_0 the initial amount of monomer per cm^3 of water, and N_A is Avogadro's number.

The population balance for N_1 is

$$\frac{dN_1}{dt} = k_a[R]_w(N_T - 2N_1) - k_d N_1 \quad (2)$$

where k_a is the entry rate coefficient, k_d the rate coefficient for radical desorption, N_T is the number of polymer particles per cm^3 of water, and $[R]_w$ the concentration of free radicals in the aqueous phase that can be calculated through the material balance for free radicals in the aqueous phase:

$$\frac{d[R]_w}{dt} = 2f k_I[I_2] + k_d \frac{N_1}{N_A} - k_a[R]_w \frac{N_T}{N_A} - 2k_{tw}[R]_w^2 \quad (3)$$

where k_I and f are the rate coefficient and the efficiency factor, respectively, for the generation of free radicals from initiator decomposition, and k_{tw} is the termination rate constant in the aqueous phase. It has been demonstrated[13] that the pseudo steady-state assumption can be safely used, and hence equation (3) can be converted into an algebraic equation by making the accumulation term of the left hand side member equal to zero. In equation (3) it is assumed that the volume of the aqueous phase is equal to the volume of water, which is acceptable for sparingly water-soluble monomers like styrene, and that the 'background' thermal production of radicals is negligible.

The material balance for the initiator is:

$$\frac{d[I_2]}{dt} = -k_I[I_2] \quad (4)$$

Model 1 includes the rate coefficients for radical entry and exit. The radical absorption phenomenon has been explained through different mechanisms. Gardon[2] treated the entry as a collisional process predicting that the radical entry rate is proportional to the square of the particle diameter. Ugelstad and Hansen[6] proposed that the rate-determining step for entry is the diffusion of soluble oligomeric species from the aqueous phase to the particle surface. In this model, a linear dependence of the entry rate coefficient on the particle diameter is predicted. Yeliseeva[8] suggested that the displacement of surfactant from the particle surface is the rate-determining step. This mechanism implies that the radical capture rate depends on the surface coverage of the latex particle by the surfactant. However, Adams *et al.*[14] found that the entry rate was virtually independent of the extent of the latex surface coverage. Penboss *et al.*[9] proposed the colloidal process, where the entering species are large insoluble colloidal entities and the rate-controlling step is based on DLVO-type colloidal considerations. The dependence of the entry rate coefficient on the particle diameter can be considered as linear.

More recently, Maxwell *et al.*[11] have postulated a new mechanism in which the propagation of the free radicals in the aqueous phase to a critical degree of polymerization is the rate-determining step for entry. This model, called propagational, predicts almost no dependence of the entry rate coefficient on the particle diameter, for a constant number of particles. However, its use in the framework of Model 1 may be inconsistent because conflicting assumptions are used: Model 1 assumes that any radical can enter into the particles, while Maxwell's model considers that only radicals of a critical length enter into the polymer particles.

Table 1 presents a summary of the dependence of the entry rate coefficient on the particle diameter predicted by the different models proposed in the literature and described above.

The early works related to radical desorption from polymer particles[1,5] assumed that excited free radicals did not reabsorb into the polymer particles. Ugelstad *et al.*[3] proposed a mechanism involving a rapid desorption and reabsorption of radicals in the latex particles in the investigation of the kinetics of vinyl chloride emulsion polymerization. Nomura and co-workers[4,7] and Asua *et al.*[10] presented an analysis of free radical exit kinetics taking into account the reabsorption of previously described single-unit monomeric radicals. However, Nomura and co-workers[4,7] considered irreversible entry of the reabsorbed radicals, whereas Asua *et al.*[10] took into account the possibility of redesorption. Asua *et al.*[10] were able to explain experimental results[15] that Nomura's model could not justify. Assuming that only single-unit radicals can desorb, Asua *et al.*[10] derived the following equation for the desorption rate coefficient:

$$k_d = k_{fm}[M]_p \frac{\left(\sum_{n=0}^{\infty} nP_n N_n / N_T\right) \Big/ \bar{n}}{\left[1 - (1-\beta)\sum_{n=0}^{\infty} P_{n+1} N_n / N_T\right]} \quad (5)$$

where k_{fm} is the monomer chain transfer rate constant, N_n the number of particles containing n radicals, P_n the probability of desorption of a monomeric radical from a particle containing n radicals, and β the probability that the desorbed monomeric radical reacts in the aqueous phase by either propagation or termination. These probabilities are given by

$$P_n = \frac{K_0}{K_0 + k_{p_1}[M]_p + 2c(n-1)} \quad (6)$$

$$\beta = \frac{k_p[M]_w + k_{tw}[R]_w}{k_p[M]_w + k_{tw}[R]_w + k_a N_T / N_A} \quad (7)$$

Table 1 Dependence of entry rate coefficient on particle diameter predicted by different models

Model	Dependence on d_p
Collisional[2]	d_p^2
Diffusional[6]	d_p
Colloidal[9]	d_p
Propagational[11]	Almost no dependence[a]

[a] For a constant number of particles

where K_0 is the rate of exit of monomeric radicals out of the particle. Assuming a diffusion mechanism and no additional resistance in the interphase, Nomura[7] derived the following equation for K_0:

$$K_0 = \frac{12(D_w/m_d)}{1 + 2(D_w/m_d D_p)} \frac{1}{d_p^2} \quad (8)$$

where D_w and D_p are the diffusion coefficients of a monomeric radical in the aqueous phase and the polymer particles, respectively, m_d is the partition coefficient of such a radical between polymer particles and aqueous phase, and d_p is the diameter of the monomer swollen polymer particles. Parameter k_{p_1} is the propagation rate constant of a monomeric radical, $[M]_w$ is the concentration of monomer in the aqueous phase, k_a is the entry rate coefficient, and c is the termination rate coefficient, given by:

$$c = k_t/v_p N_A \quad (9)$$

where k_t is the termination rate constant in the polymer particles and v_p is the volume of the swollen particle.

Unless very small particles are involved, P_n remains constant for low values of n and equation (5) reduces to[10]:

$$k_d = k_{fm}[M]_p \frac{K_0}{\beta K_0 + k_{p_1}[M]_p} \quad (10)$$

For sparingly water-soluble monomers $\beta \to 0$, whereas for highly water-soluble monomers $\beta \to 1$. In addition, if the exit occurs by diffusion with no additional resistance in the interface, K_0 is inversely proportional to the square of the particle diameter[7]. Therefore:

$$k_d \div \frac{1}{d_p^2} \quad \text{if} \quad k_{p_1}[M]_p \gg \beta K_0 \quad (11)$$

$$k_d \neq f(d_p) \quad \text{if} \quad k_{p_1}[M]_p \ll \beta K_0 \quad (12)$$

The propagation rate constant of a monomeric radical, k_{p_1}, is expected to be higher than the average propagation rate constant. In addition, for sparingly water soluble monomers like styrene, both β and K_0 should be low and the limit given by equation (11) likely applies.

Casey *et al.*[12] claiming that the previous models did not account properly for the differences between initiator derived radicals and monomeric radicals, have proposed a detailed model for radical exit that includes different population balances for particles containing monomeric radicals and particles with longer radicals. However, Barandiaran and Asua[16] have demonstrated that the complicated equations developed by Casey *et al.*[12] can be reduced to equation (5) because the distinction between initiator derived radicals and monomeric radicals was properly accounted for in equation (5). In this paper, the simplified expression for k_d given by equation (10) was used.

Model 2

Model 2 does make distinction between initiator-derived radicals and transfer-derived radicals in the aqueous phase. It is worth stressing that this distinction affects only the entry mechanism because this difference is already included in the exit model developed by Asua *et al.*[10].

The initiator-derived free radicals are produced in the aqueous phase and irreversible entry into the polymer particles is considered to be negligible if the length of the radical is less than a critical value, z. This minimum length of the hydrophobic chain is required to overcome the effect of the inorganic part resulting from the initiator. Two alternative submodels are used based on the different mechanisms proposed for initiator-derived free radicals of length $\geq z$. In submodel 2a, it is assumed that the initiator derived free radical of length $\geq z$ can either enter into the polymer particles, propagate in the aqueous phase or terminate in this phase. In this submodel, monomer chain transfer derived radicals of any length can be absorbed into the polymer particles because they do not contain inorganic parts. The submodel 2b corresponds to the propagational entry model proposed by Maxwell *et al.*[11]. These authors postulated that instantaneous entry occurs when the initiator derived oligoradicals become surface active by reaching the critical degree of polymerization, z. The monomer chain transfer-derived radicals that appear in the aqueous phase by desorption from the polymer particles have no inorganic part and hence, oligoradicals of any length can enter into the polymer particles. In the frame of submodel 2b, a critical length for irreversible entry of these radicals is required. This critical length has been assumed to be 2, that is likely to be an upper limit for aqueous solubility of polystyrene oligomers.

The pseudo steady state balances for initiator-derived radicals in the aqueous phase are:

$$\frac{d[I^\circ]}{dt} = 0 = 2f k_I[I_2] - k_{p_{I1}}[I^\circ][M]_w - 2k_{tw}[I^\circ][T^\circ] \quad (13)$$

$$\frac{d[IM_1^\circ]}{dt} = 0 = k_{p_{I1}}[I^\circ][M]_w - k_p[IM_1^\circ][M]_w - 2k_{tw}[IM_1^\circ][T^\circ] \quad (14)$$

$$\frac{d[IM_i^\circ]}{dt} = 0 = k_p[IM_{i-1}^\circ][M]_w - k_p[IM_i^\circ][M]_w - 2k_{tw}[IM_i^\circ][T^\circ] \quad (2 \leq i < z) \quad (15)$$

The $[IM_j^\circ]$ balance for $j \geq z$ depends on the entry mechanism considered. For submodel 2a, which does not consider instantaneous entry of initiator derived radicals of critical length, the material balance for $[IM_j^\circ]$ is:

$$\frac{d[IM_j^\circ]}{dt} = 0 = k_p[IM_{j-1}^\circ][M]_w - k_p[IM_j^\circ][M]_w - 2k_{tw}[IM_j^\circ][T^\circ] - k_{a_1}^{(j)}[IM_j^\circ]\frac{N_T}{N_A} \quad (j \geq z) \quad (16a)$$

whereas for submodel 2b (propagational entry mechanism), it is:

$$[IM_j^\circ] = 0 \quad (j \geq z) \quad (16b)$$

In equation (16a), the entry rate coefficients can be both radical length dependent and particle size dependent. Taking into account the relationship between the diffusion coefficient and the molecular volume proposed by Wilke and Chang [17], the entry rate coefficients can be written as follows:

$$k_{a_1}^{(j)} = k_{a_1}^* \frac{d_p^{\alpha_1}}{j^{0.6}} \quad (17)$$

For a 'zero–one' system, submodel 2a (any radical can either absorb into the particles or propagate or terminate in the aqueous phase) leads to the following pseudo steady-state balances for the transfer-derived radicals in the aqueous phase:

$$\frac{d[M_1^\circ]}{dt} = 0 = k_d \frac{N_1}{N_A} - k_{p_1}[M_1^\circ][M]_w - 2k_{tw}[M_1^\circ][T^\circ] - k_{a_m}^{(1)}[M_1^\circ]\frac{N_T}{N_A} \quad (18)$$

$$\frac{d[M_n^\circ]}{dt} = 0 = k_p[M_{n-1}^\circ][M]_w - k_p[M_n^\circ][M]_w - 2k_{tw}[M_n^\circ][T^\circ] - k_{a_m}^{(n)}[M_n^\circ]\frac{N_T}{N_A} \quad (n \geq 2) \quad (19)$$

For a 'zero–one' system, model 2b gives:

$$\frac{d[M_1^\circ]}{dt} = 0 = k_d \frac{N_1}{N_A} - k_{p_1}[M_1^\circ][M]_w - 2k_{tw}[M_1^\circ][T^\circ] - k_{a_m}^{(1)}[M_1^\circ]\frac{N_T}{N_A} \quad (20)$$

Notice that chain length dependent entry rate coefficients are used in equations (18), (19) and (20). These coefficients can be written as follows:

$$k_{a_m}^{(n)} = k_{a_m}^* \frac{d_p^{\alpha_1}}{n^{0.6}} \quad (21)$$

The total concentration of free radicals in the aqueous phase for submodel 2a is:

$$[T^\circ] = \sum_{i=1}^{\infty}[IM_i^\circ] + \sum_{n=1}^{\infty}[M_n^\circ] + [I^\circ] \quad (22a)$$

whereas for submodel 2b it is:

$$[T^\circ = \sum_{i=1}^{z-1}[IM_i^\circ] + \sum_{n=1}^{z-1}[M_n^\circ] + [I^\circ] \quad (22b)$$

For a 'zero–one' system the population balance of particles with one radical is as follows:

$$\frac{dN_1}{dt} = \left\{\sum_{n=1}^{\infty} k_{a_m}^{(n)}[M_n^\circ] + \sum_{i=z}^{\infty} k_{a_1}^{(i)}[IM_i^\circ]\right\} \times (N_T - 2N_1) - k_d N_1 \quad (23a)$$

$$\frac{dN_1}{dt} = \left\{k_{a_m}^{(1)}[M_1^\circ] + (k_{p_1}[M_1^\circ][M]_w + k_p[IM_{z-1}][M]_w)\frac{N_A}{N_T}\right\} \times (N_T - 2N_1) - k_d N_1 \quad (23b)$$

where equation (23a) corresponds to the submodel 2a and equation (23b) to the submodel 2b.

The material balances for the monomer and the initiator are the same as in Model 1 (equations (1) and (4)).

EXPERIMENTAL

Styrene was purified by distillation under reduced pressure and stored at −18°C until used. $K_2S_2O_8$ (Merck), $Na_2S_2O_8$ (Merck), $NaHCO_3$ (Merck), Aerosol MA-80 (sodium dihexyl sulfosuccinate, Cyanamid) and sodium lauryl sulfate (SLS, Henkel) were used as received. Deionized water was used throughout the work.

Three monodisperse seed latexes were prepared at 90°C in a batch reactor using the recipes presented in *Table 2*. *Table 3* presents the seed diameter as measured by transmission electron microscopy (TEM). Before being used in the kinetic runs, the seeds were cleaned by dialysis. Kinetic runs were conducted at 60°C under Interval II conditions in a calorimeter reactor (Chemisens–Thermometric RM-1). Prior to the polymerization, the seed was swollen in the reactor at room temperature during 15 h. In addition, the thermal stabilization and the calibration of the calorimeter reactor required 2.5 h at the reaction temperature. Both swelling and thermal stabilization and calibration were carried out under nitrogen blanket. The flow rate of N_2 (purity 99.999%) was chosen to evacuate 62 times the headspace of the reactor. Before injecting the initiator, a sample was

Table 2 Recipes used for the preparation of polystyrene seeds

Seed	Styrene (g)	MA-80 (g)	H_2O (g)	$NaHCO_3$ (g)	$K_2S_2O_8$ (g)
SL1	403	20.47	959	1.5	1.5
SL2	97	14.99	1027	1.0	1.0
SL3	422	17.14	1026	1.6	1.6

Table 3 Seeds used in the present work

Seed	d_p (nm)	PDI	CV (%)
SL1	79	1.017	8.39
SL2	100	1.012	6.92
SL3	117	1.007	4.96

Table 4 Summary of the kinetic runs

Seed	N_T (particles cm^{-3} of water)	$[Na_2S_2O_8]$ (mol cm^{-3} of water)
SL1	14.5×10^{13}	0.6×10^{-7}
		1.2×10^{-7}
		2.6×10^{-7}
		5.1×10^{-7}
		10.4×10^{-7}
		20.7×10^{-7}
	28.7×10^{13}	1.3×10^{-7}
		2.6×10^{-7}
		5.2×10^{-7}
		10.4×10^{-7}
SL2	5.5×10^{13}	2.6×10^{-7}
		4.9×10^{-7}
		10.5×10^{-7}
		37.2×10^{-7}
	11.0×10^{13}	2.6×10^{-7}
		5.1×10^{-7}
		10.4×10^{-7}
		21.1×10^{-7}
	22.6×10^{13}	5.2×10^{-7}
		20.3×10^{-7}
SL3	4.6×10^{13}	5.2×10^{-7}
		10.6×10^{-7}
	7.9×10^{13}	1.3×10^{-7}
		2.6×10^{-7}
		10.5×10^{-7}
	11.9×10^{13}	5.4×10^{-7}
	15.9×10^{13}	1.3×10^{-7}
		2.6×10^{-7}
		5.2×10^{-7}

withdrawn from the reactor and its conversion determined by gravimetry to check for thermal polymerization. In all runs thermal polymerization was observed, its extent varying widely, but corresponding to a negligible polymerization rate as compared to those recorded during most of the kinetics runs. The monomer consumed by thermal polymerization was taken into account to calculate the actual particle diameter and monomer concentration at the beginning of the process.

Table 5 Parameter values taken from literature

k_I [21]	$5.8 \times 10^{-6}\ s^{-1}$
f [21]	0.6
k_p [22]	$3.76 \times 10^5\ cm^3\ mol^{-1}\ s^{-1}$
k_{tw} [23]	$7 \times 10^{10}\ cm^3\ mol^{-1}\ s^{-1}$
k_{fm} [24]	$8.8\ cm^3\ mol^{-1}\ s^{-1}$
$[M]_p$ [2]	$5.01 \times 10^{-3}\ mol\ cm^{-3}$
$[M]_w$ [25]	$5.1 \times 10^{-6}\ mol\ cm^{-3}$

The kinetic runs were started by injecting into the reactor an aqueous solution of the initiator. Polymerizations were carried out under a nitrogen blanket. All the polymerizations were examined by TEM to check for new nucleations. Polymerizations with new nucleations were rejected. *Table 4* presents a summary of the polymerizations carried out in which the number of polymer particles and the concentration of initiator were varied for each seed.

PARAMETER ESTIMATION AND MODEL DISCRIMINATION

The models contained several parameters whose values can be obtained from literature. *Table 5* lists these parameters and their values. It has to be pointed out that k_{tw} was assumed to be equal to the termination rate constant at zero polymer content and that k_{p_I} and $k_{p_{II}}$ were set equal to k_p. The rest of the parameters of the

Table 6 Values of k_a and k_d estimated for each seed using model 1

d_p (nm)[a]	k_a ($cm^3\ mol^{-1}\ s^{-1}$)	k_d (s^{-1})	ε
79	$0.37 \times 10^{10} \pm 0.24 \times 10^8$	$1.4 \times 10^{-2} \pm 0.44 \times 10^{-3}$	2.2×10^{-5}
100	$0.47 \times 10^{10} \pm 0.61 \times 10^9$	$1.2 \times 10^{-2} \pm 0.11 \times 10^{-2}$	9.5×10^{-6}
117	$0.55 \times 10^{10} \pm 0.12 \times 10^{10}$	$9.8 \times 10^{-3} \pm 1.09 \times 10^{-3}$	4.1×10^{-5}

[a] Unswollen seed particle diameter

Table 7 Values of the entry and exit rate coefficient estimated assuming different size dependences

α_1	α_2	k_a^*	k_a ($d_p = 150$ nm)	k_d^*	k_d ($d_p = 150$ nm)	ε
1	0	0.32×10^{15}	4.80×10^9	1.24×10^{-2}	1.24×10^{-2}	2.86×10^{-5}
1	0.5	0.31×10^{15}	4.65×10^9	0.46×10^{-4}	1.19×10^{-2}	2.49×10^{-5}
1	1	0.32×10^{15}	4.80×10^9	1.74×10^{-7}	1.16×10^{-2}	2.47×10^{-5}
1	1.5	0.34×10^{15}	5.10×10^9	6.67×10^{-10}	1.15×10^{-2}	2.79×10^{-5}
1	2	0.38×10^{15}	5.70×10^9	2.59×10^{-12}	1.15×10^{-2}	3.43×10^{-5}
2	0	20.63×10^{18}	4.64×10^9	1.16×10^{-2}	1.16×10^{-2}	2.52×10^{-5}
2	0.5	24.07×10^{18}	5.41×10^9	0.47×10^{-4}	1.21×10^{-2}	2.49×10^{-5}
2	1	28.57×10^{18}	6.43×10^9	1.90×10^{-7}	1.27×10^{-2}	2.77×10^{-5}
2	1.5	34.28×10^{18}	7.72×10^9	7.61×10^{-10}	1.31×10^{-2}	3.29×10^{-5}
2	2	41.91×10^{18}	9.43×10^9	3.02×10^{-12}	1.34×10^{-2}	4.05×10^{-5}

Table 8 Values of $k_{a_I}^*$, $k_{a_m}^*$ and k_d^* estimated for submodel 2a

z	α_1	α_2	$k_{a_m}^*$	$k_{a_I}^*$	k_d^*	ε
2	1	2	6.37×10^{17}	3.19×10^{16}	1.51×10^{-12}	3.46×10^{-5}
2	1	1	7.13×10^{17}	3.48×10^{16}	1.45×10^{-7}	2.82×10^{-5}
2	1	0	7.11×10^{17}	3.98×10^{16}	1.40×10^{-2}	3.25×10^{-5}
2	2	2	4.75×10^{24}	1.43×10^{24}	1.99×10^{-12}	4.36×10^{-5}
2	2	1	4.21×10^{24}	1.88×10^{24}	1.86×10^{-7}	3.60×10^{-5}
2	2	0	4.88×10^{24}	2.17×10^{24}	1.74×10^{-2}	3.89×10^{-5}
3	1	2	8.69×10^{17}	1.27×10^{17}	1.32×10^{-12}	4.77×10^{-5}
3	1	1	9.79×10^{17}	1.35×10^{17}	1.25×10^{-7}	3.97×10^{-5}
3	1	0	9.89×10^{17}	3.40×10^{17}	1.24×10^{-2}	4.22×10^{-5}
3	2	2	5.68×10^{24}	2.12×10^{24}	1.45×10^{-12}	4.87×10^{-5}
3	2	1	7.86×10^{24}	2.61×10^{24}	1.38×10^{-7}	4.04×10^{-5}
3	2	0	5.61×10^{24}	2.33×10^{24}	1.27×10^{-2}	4.24×10^{-5}

different models were estimated by minimizing the residual sum of squares.

Model 1

Taking into account the parameters listed in *Table 5*, only the entry and exit rate coefficient remain to be estimated. Because these parameters depend on the particle diameter and the three sets of experiments were carried out using seeds of different size, each set was treated separately. Parameter estimation was carried out using the approach proposed by Asua and co-workers[13,18] assuming that the particle size did not vary during polymerization. *Table 6* presents the values of k_a and k_d estimated for each seed. In this table, ε is the square error per experimental point, namely, the sum of square errors divided by the number of experimental points considered. The value of ε is a measure of the agreement between experimental data and model predictions. *Table 6* shows that k_a increased and k_d decreased when the unswollen seed diameter increased from 79 to 117 nm. Parameter k_a was proportional to the particle diameter, d_p, which is consistent with both diffusional[6] and colloidal[9] entry mechanisms. On the other hand, k_d was inversely proportional to the 0.88th power of d_p. This power is lower than the expected one (see equation (5)). However, some error can be introduced by neglecting the variation of the particle size during polymerization[19].

In order to take into account the variation of the parameters during the polymerization, the entry and exit rate coefficients were rewritten as follows:

$$k_a = k_a^* d_p^{\alpha_1} \tag{24}$$

$$k_d = k_d^* d_p^{-\alpha_2} \tag{25}$$

where k_a^* and k_d^* include all the components of k_a and k_d, respectively, but the particle diameter dependence. α_1 can vary between 1 and 2, depending on the model chosen (see *Table 1*) and α_2 between 0 and 2, depending on the solubility of the monomers in water (see equations (11) and (12)). Parameters k_a^* and k_d^* were estimated using the approach proposed by Asua and co-workers[13,18] and different values of α_1 and α_2. The results are presented in *Table 7* where it can be seen that the best fitting (minimum value of ε) was obtained for $\alpha_1 = 1$ and $\alpha_2 = 1$. Although these values are only approximate because α_1 and α_2 were not estimated but discrete values were used, they confirm that k_a was proportional to d_p and k_d was inversely proportional to a power close to one. As explained above, the dependence of k_a on d_p is consistent with both diffusional[6] and colloidal[9] entry mechanisms. However, the dependence of k_d on d_p was lower than what was expected (see equation (5)). This result might be simply due to the fact that the mathematical model used was too simple to account for the complexities of emulsion polymerization. Therefore, the other models were used to fit the data. The confidence intervals of k_a^* and k_d^* for $\alpha_1 = 1$ and $\alpha_2 = 1$ are

$$k_a^* = 0.32 \times 10^{15} \pm 2.57 \times 10^{13} \tag{26}$$

$$k_d^* = 1.74 \times 10^{-7} \pm 8.06 \times 10^{-9} \tag{27}$$

Model 2

As has been explained above, Model 2 has been divided into two submodels: submodel 2a that does not consider instantaneous entry of initiator-derived radicals of critical length, and assumes that transfer-derived radicals in the aqueous phase can either absorb into polymer particles or propagate or terminate in the aqueous phase; and submodel 2b, that considers the

Table 9 Values of $k_{a_m}^*$ and k_d^* estimated for submodel 2b

z	α_1	α_2	$k_{a_m}^*$	k_d^*	ε
2	1	2	6.62×10^{17}	1.44×10^{-12}	4.87×10^{-5}
2	1	1	4.65×10^{17}	1.38×10^{-7}	4.04×10^{-5}
2	1	0	2.48×10^{16}	1.21×10^{-2}	4.18×10^{-5}
2	2	2	5.93×10^{24}	1.45×10^{-12}	4.87×10^{-5}
2	2	1	7.15×10^{22}	1.39×10^{-7}	4.04×10^{-5}
2	2	0	6.52×10^{22}	1.27×10^{-2}	4.25×10^{-5}
3	1	2	1.69×10^{17}	7.52×10^{-13}	9.77×10^{-5}
3	1	1	8.52×10^{16}	7.12×10^{-8}	8.89×10^{-5}
3	1	0	1.09×10^{17}	6.42×10^{-3}	8.84×10^{-5}
3	2	2	4.19×10^{24}	5.00×10^{-13}	1.20×10^{-4}
3	2	1	4.19×10^{24}	7.25×10^{-8}	8.77×10^{-5}

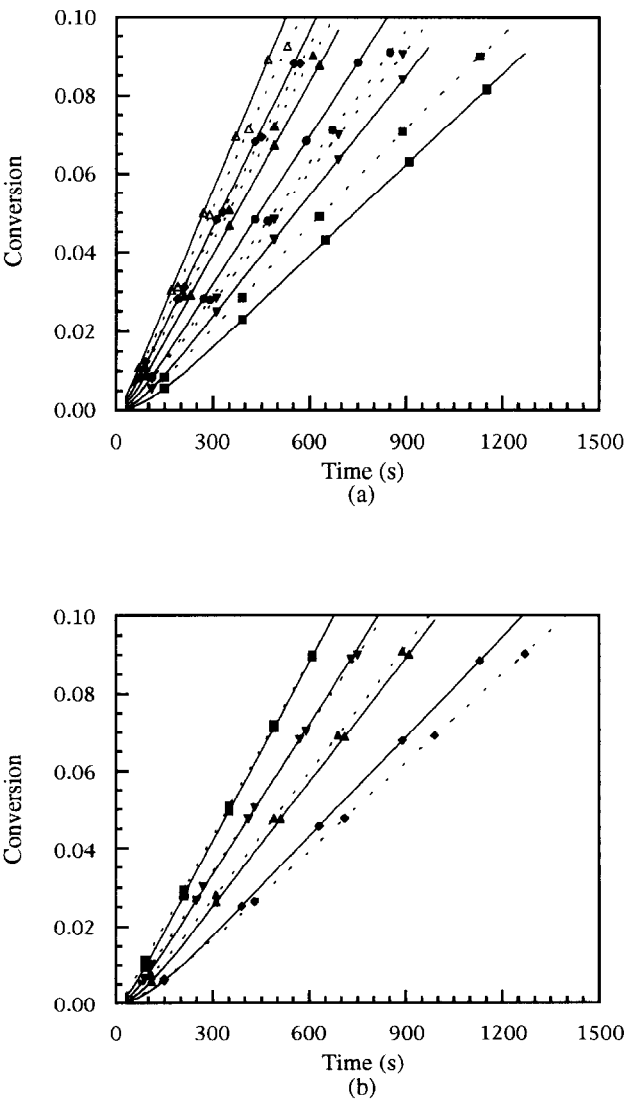

Figure 1 Comparison between experimental results (– – –) and model predictions (——) for seed SL1. (a) $N_T = 14.5 \times 10^{13}$ part cm^{-3} of water, $[I_2] \times 10^7$ mol cm^{-3} of water: (■) 0.6; (▼) 1.2; (●) 2.6; (▲) 5.1; (◆) 10.4; (△) 20.7. (b) $N_T = 28.7 \times 10^{13}$ part cm^{-3} of water, $[I_2] \times 10^7$ mol cm^{-3} of water: (◆) 1.3; (▲) 2.6; (▼) 5.2; (■) 10.4

propagational entry mechanism (instantaneous entry of initiator-derived radicals of critical length), and that only monomeric radicals of length 1 can exist in the aqueous phase.

The parameters to be estimated in submodel 2a are $k_{p_{I_1}}$, k_{p_I}, z, $k^*_{a_I}$, $k^*_{a_m}$ and k_d. The sensitivity of the model to the propagation rate constants is low and no attempts to estimate them from the data were carried out. In addition, although both $k_{p_{I_1}}$ and k_{p_I} are expected to be higher than the average propagation rate constant, no values of them are available in literature, and hence $k_{p_{I_1}}$ and k_{p_I} were set equal to k_p. On the other hand, k_d was expressed as in equation (25).

$k^*_{a_I}$, $k^*_{a_m}$ and k^*_d were estimated by means of the approach proposed by Asua *et al.*[13,18] for different values of α_1, α_2 and z and using all of the experimental data at the same time. *Table 8* presents the values of the estimated parameters and the square error per experimental point achieved for different values of α_1, α_2 and z using submodel 2a, which does not consider instantaneous entry of initiator-derived free radical of critical length. It can be seen that the best fit was achieved with $\alpha_1 = 1$, $\alpha_2 = 1$ and $z = 2$. For these values, the confidence intervals of $k^*_{a_m}$, $k^*_{a_I}$ and k^*_d are as follows:

$$k^*_{a_m} = 7.13 \times 10^{17} \pm 1.68 \times 10^{16} \quad (28)$$

$$k^*_{a_I} = 3.48 \times 10^{16} \pm 3.5 \times 10^{14} \quad (29)$$

$$k^*_d = 1.45 \times 10^{-7} \pm 4.76 \times 10^{-10} \quad (30)$$

Using similar assumptions as in submodel 2a, the parameters to be estimated in submodel 2b are z, $k^*_{a_m}$ and k^*_d. *Table 9* presents the values of $k^*_{a_m}$ and k^*_d estimated for different values of α_1, α_2 and z, using submodel 2b in which the entry of initiator-derived free radicals of critical length is considered. It can be seen that the best fit was also achieved with $\alpha_1 = 1$, $\alpha_2 = 1$ and $z = 2$. For these values, the confidence intervals of $k^*_{a_m}$ and k^*_d are:

$$k^*_{a_m} = 4.65 \times 10^{17} \pm 2.68 \times 10^{16} \quad (31)$$

$$k^*_d = 1.38 \times 10^{-7} \pm 5.39 \times 10^{-9} \quad (32)$$

Comparison of the smallest values of ε obtained with the three models (*Tables 7*, *8* and *9*) indicates that a

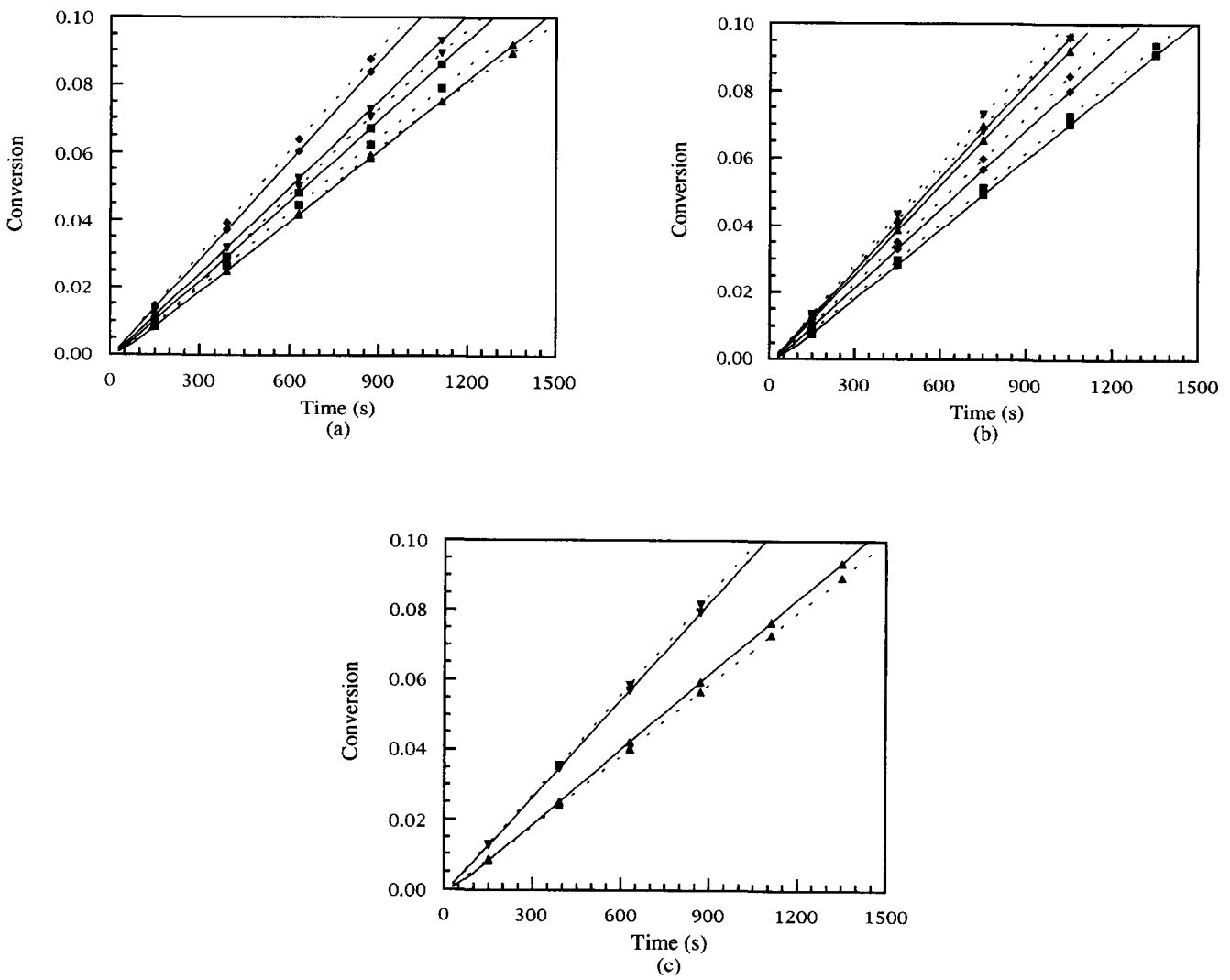

Figure 2 Comparison between experimental results (– – –) and model predictions (——) for seed SL2. (a) $N_T = 5.5 \times 10^{13}$ part cm^{-3} of water, $[I_2] \times 10^7$ mol cm^{-3} of water: (▲) 2.6; (■) 4.9; (▼) 10.5; (◆) 37.2. (b) $N_T = 11 \times 10^{13}$ part cm^{-3} of water, $[I_2] \times 10^7$ mol cm^{-3} of water: (■) 2.6; (◆) 5.1; (▲) 10.4; (▼) 21.1. (c) $N_T = 22.6 \times 10^{13}$ part cm^{-3} of water, $[I_2] \times 10^7$ mol cm^{-3} of water: (▲) 5.2; (▼) 20.3

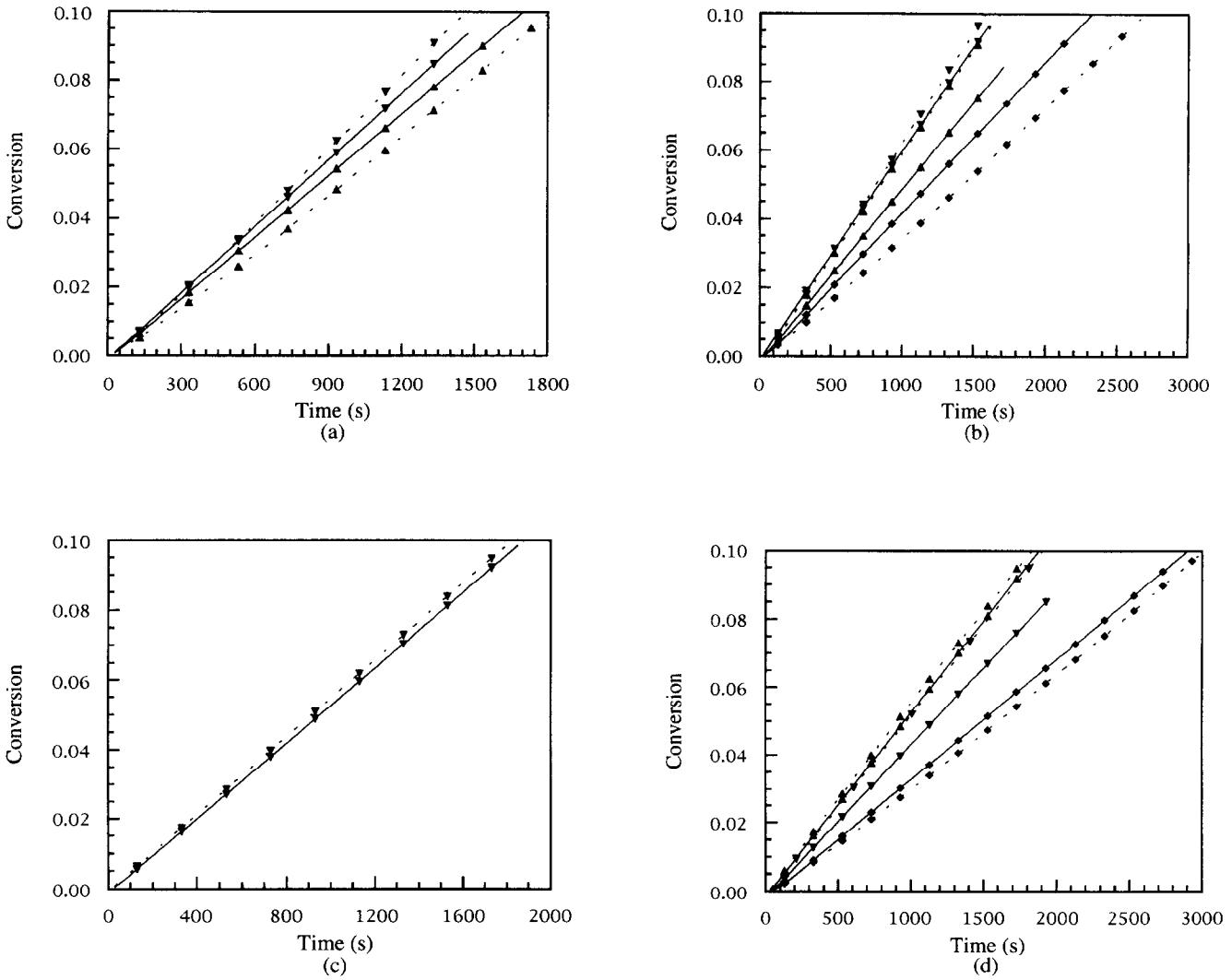

Figure 3 Comparison between experimental results (– – –) and model predictions (——) for seed SL3. (a) $N_T = 4.6 \times 10^{13}$ part cm^{-3} of water, $[I_2] \times 10^7$ mol cm^{-3} of water: (▲) 5.2; (▼) 10.6. (b) $N_T = 7.9 \times 10^{13}$ part cm^{-3} of water, $[I_2] \times 10^7$ mol cm^{-3} of water: (◆) 1.3; (▲) 2.6; (▼) 10.5. (c) $N_T = 11.9 \times 10^{13}$ part cm^{-3} of water, $[I_2] \times 10^7$ mol cm^{-3} of water: (▼) 5.4. (d) $N_T = 15.9 \times 10^{13}$ part cm^{-3} of water, $[I_2] \times 10^7$ mol cm^{-3} of water: (◆) 1.3; (▼) 2.6; (▲) 5.2

similar fit was obtained with the three models giving Model 2b a slightly worse fit than the others. Nevertheless, the χ^2 test showed that the fit of the models were equivalent from a statistical point of view. *Figures 1–3* present the comparison between experimental results and the predictions of Model 1. It has to be stressed that the three models predicted the same values for α_1, α_2 and z. The value of $z = 2$ agrees with the length required for an initiator derived styrene radical to become surface active[11], and the value of $\alpha_1 = 1$ is consistent with both diffusional[6] and colloidal[9] entry mechanisms. However, the dependence of k_d on d_p was lower than what was expected for a sparingly water soluble monomer such as styrene (equation (5)). A possible explanation of this result is that, contrary to what was implicitly assumed in the models, radical concentration in the polymer particles was not uniform but a concentration profile exists due to the anchoring of the entering initiator-derived radicals to the surface of the polymer particle. de la Cal *et al.*[20] showed that the more pronounced the radical concentration profile, the higher the rate for radical desorption. Larger particles have more pronounced radical concentration profiles, and hence comparatively faster radical desorptions that can counteract the effect of d_p on k_d predicted by equation (5) leading to a lower value of α_2. This hypothesis will be further investigated in a future work because it may cast doubt upon the existing approaches for kinetic investigation of emulsion polymerization systems.

CONCLUSIONS

An attempt to develop a predictive and manageable mathematical model for particle growth in emulsion polymerization was carried out. To achieve this goal, mathematical models of different levels of complexity were used to fit the time evolution of the conversion during the approach to the steady state values of $\bar{n}$ in the chemically initiated seeded emulsion polymerization of styrene carried out under a wide range of experimental conditions. The mathematical models used differed in the detail used to describe the radicals in the aqueous phase. The simplest model (Model 1) made no distinction

between radicals in the aqueous phase, whereas Model 2 distinguished between initiator-derived radicals and transfer-derived radicals in the aqueous phase. Model 2 was subdivided into submodel 2a that does not consider instantaneous entry of initiator-derived radicals of critical length and submodel 2b that considered instantaneous entry of these radicals. It was found that the three models fitted in a similar way the experimental data, submodel 2b giving a slightly worse fit, although the three models were statistically equivalent. No advantage was observed by increasing the complexity of the mathematical model by including the distinction between initiator-derived radicals and transfer-derived radicals in the aqueous phase.

The dependence of the entry rate coefficient on the particle size is consistent with both diffusional[6] and colloidal[9] entry mechanisms. On the other hand, the dependence of k_d on the particle diameter suggest that the anchoring of the initiator-derived radicals on the surface of the polymer particle might have a significant role on the desorption mechanisms. This will be further investigated in a future paper because it may cast doubt upon the existing approaches for kinetic investigation of emulsion polymerization systems.

ACKNOWLEDGEMENTS

The financial support by the Diputación Foral de Gipuzkoa and the CICYT (grant MAT 94-0002) are gratefully appreciated. Lourdes López de Arbina and Luis M. Gugliotta acknowledge the fellowships from the Basque Government and the CONICET, respectively.

NOMENCLATURE

c Termination rate coefficient (s^{-1})
CV Coefficient of variation
D_w Diffusion coefficient of a monomeric radical in the aqueous phase ($cm^2\ s^{-1}$)
D_p Diffusion coefficient of a monomeric radical in the polymer particles ($cm^2\ s^{-1}$)
d_p Diameter of the swollen polymer particle (cm)
f Efficiency factor for initiator decomposition
$[I_2]$ Concentration of initiator ($mol\ cm^{-3}$)
$[I^\circ]$ Concentration of radicals formed by homolytic decomposition of initiator ($mol\ cm^{-3}$)
$[IM_i^\circ]$ Concentration of species resulting after i propagation events of I° in the aqueous phase ($mol\ cm^{-3}$)
k_a Entry rate coefficient ($cm^3\ mol^{-1}\ s^{-1}$)
k_a^* Parameter defined by equation (24)
$k_{a_1}^j$ Entry rate coefficient of initiator-derived radical of length j ($cm^3\ mol^{-1}\ s^{-1}$)
$k_{a_1}^*$ Parameter defined by equation (17)
$k_{a_m}^n$ Entry rate coefficient of transfer-derived radical of length n ($cm^3\ mol^{-1}\ s^{-1}$)
$k_{a_m}^*$ Parameter defined by equation (21)
k_d Desorption rate coefficient (s^{-1})
k_d^* Parameter defined by equation (25)
k_{fm} Monomer chain transfer constant ($cm^3\ mol^{-1}\ s^{-1}$)
k_I Rate coefficient for initiator decomposition (s^{-1})
k_p Propagation rate constant ($cm^3\ mol^{-1}\ s^{-1}$)
k_{p_1} Propagation rate constant of a monomeric radical ($cm^3\ mol^{-1}\ s^{-1}$)
$k_{p_{11}}$ Propagation rate constant in the aqueous phase of I° ($cm^3\ mol^{-1}\ s^{-1}$)
k_t Termination rate constant ($cm^3\ mol^{-1}\ s^{-1}$)
k_{tw} Termination rate constant in the aqueous phase ($cm^3\ mol^{-1}\ s^{-1}$)
K_0 Rate of exit of a monomeric radical from a polymer particle (s^{-1})
$[M]_p$ Monomer concentration in the polymer particles ($mol\ cm^{-3}$)
$[M]_w$ Monomer concentration in the aqueous phase ($mol\ cm^{-3}$)
M_0 Amount of monomer initially charged into the reactor ($mol\ cm^{-3}$)
$[M_i^\circ]$ Concentration of transfer-derived radicals of length i ($mol\ cm^{-3}$)
$\bar{n}$ Average number of radicals per particle
m_d Partition coefficient of a radical between polymer particles and aqueous phase
N_1 Number of polymer particles containing one radical, per cm^3 of water
N_A Avogadro's number
N_n Number of polymer particles containing n radicals, per cm^3 of water
N_T Total number of polymer particles, per cm^3 of water
PDI Polydispersity index
$[R]_w$ Concentration of radicals in the aqueous phase ($mol\ cm^{-3}$)
$[T^\circ]$ Total concentration of free radicals in the aqueous phase ($mol\ cm^{-3}$)
v_p Volume of the swollen polymer particle (cm^3)
x Conversion
z Critical degree of polymerization of oligomers in the aqueous phase.

Greek symbols

α_1, α_2 Parameters defined by equations (24) and (25)
β Probability that a desorbed single-unit monomeric radical reacts in the aqueous phase by either propagation or termination
ε Average residual sum of squares per point.

REFERENCES

1 O'Toole, J. T. *J. Appl. Polym. Sci.* 1965, **9**, 1291
2 Gardon, J. L. *J. Polym. Sci., Part A-1* 1968, **6**, 643
3 Ugelstad, J., Mork, P. C., Dahl, P. and Rangnes, P. *J. Polym. Sci., Part C* 1969, **27**, 49
4 Nomura, M., Harada, H., Nakagawara, K., Eguchi, W. and Nagata, S. *J. Chem. Eng. Jpn.* 1971, **4**, 160
5 Friis, N. and Nyhagen, M. *J. Appl. Polym. Sci.* 1973, **17**, 2311
6 Ugelstad, J. and Hansen, F. K. *Rubber Chem. Tech.* 1976, **49**, 536
7 Nomura, M. in 'Emulsion Polymerization' (Ed. I. Piirma), Academic Press, New York, 1982, Ch. 5
8 Yeliseeva, V. I. in 'Emulsion Polymerization' (Ed. I. Piirma), Academic Press, New York, 1982, Ch. 7
9 Penboss, I. A., Gilbert, R. G. and Napper, D. H. *J. Chem. Soc., Faraday Trans. I* 1983, **79**, 1257
10 Asua, J. M., Sudol, E. D. and El-Aasser, M. S. *J. Polym. Sci., Polym. Chem. Edn* 1989, **27**, 3903
11 Maxwell, I. A., Morrison, B. R., Napper, D. H. and Gilbert, R. G. *Macromolecules* 1991, **24**, 1629
12 Casey, B. S., Morrison, B. R., Maxwell, I. A., Gilbert, R. G. and Napper, D. H. *J. Polym. Sci., Polym. Chem. Edn* 1994, **32**, 605
13 Asua, J. M., Adams, M. E. and Sudol, E. D. *J. Appl. Polym. Sci.* 1990, **39**, 1183

14 Adams, M. E., Trau, M., Gilbert, R. G., Napper, D. H. and Sangster, D. F. *Aust. J. Chem.* 1988, **41**, 1799
15 Adams, M. E., Napper, D. H., Gilbert, R. G. and Sangster, D. F. *J. Chem. Soc., Faraday Trans. I* 1986, **82**, 1979
16 Barandiaran, M. J. and Asua, J. M., *J. Polym. Sci., Part A: Polym. Chem.* 1996, **34**, 309
17 Wilke, C. R. and Chang, P. *AIChE J.* 1955, **1**, 264
18 Barandiaran, M. J., Adams, M. E., de la Cal, J. C., Sudol, E. D. and Asua, J. M. *J. Appl. Polym. Sci.* 1992, **45**, 2187
19 de la Cal, J. C., Adams, M. E. and Asua, J. M. *Makromol. Chem., Macromol. Symp.* 1990, **35/36**, 23
20 de la Cal, J. C., Urzay, R., Zamora, A., Forcada, J. and Asua, J. M. *J. Polym. Sci., Polym. Chem. Edn* 1990, **28**, 1011
21 Blackey, D. C. 'Emulsion Polymerization', Applied Science, London, 1975, chapter 6
22 Buback, M., García-Rubio, L. H., Gilbert, R. G., Napper, D. H., Guillot, J., Hamielec, A. E., Hill, D., O'Driscoll, K. F., Olaj, O., Shen, J., Solomon, D., Moad, G., Stickler, M., Tirrell, M. and Winnik, M. A. *J. Polym. Sci., Polym. Lett. Edn* 1988, **26**, 293
23 Matheson, M. S., Auer, E. E., Bevilacqua, E. B. and Hart, E. J. *J. Am. Chem. Soc.* 1951, **73**, 1700
24 Mead, R. M. and Poehlein, G. W. *J. Appl. Polym. Sci.* 1989, **38**, 105
25 Maxwell, I. A., Morrison, B. R., Napper, D. H. and Gilbert, R. G. *Makromol. Chem.* 1992, **93**, 303